Cagelike Si_{12} clusters with endohedral Cu, Mo, and W metal atom impurities

F. Hagelberg,[1] C. Xiao,[1] and William A. Lester, Jr.[2]
[1]*Computational Center for Molecular Structure and Interactions, Department of Physics, ATM Sciences and General Science, Jackson State University, Jackson, Mississippi 39217*
[2]*Kenneth S. Pitzer Center for Theoretical Chemistry, Department of Chemistry, University of California at Berkeley, Berkeley, California 94720-1460*

(Received 12 March 2002; revised manuscript received 9 September 2002; published 31 January 2003)

In a recent series of mass-spectrometric ion trap measurements [H. Hiura *et al.*, Phys. Rev. Lett. **86**, 1733 (2001)], the formation of silicon clusters with endohedral transition-metal impurities was observed. Particular stability was assigned to the experimentally detected species WSi_{12}^+, which has been shown by *ab initio* geometry optimization to adopt the shape of a regular hexagonal Si_{12} prism with the W atom in the center. A similar geometry—namely, a Si_{12} double-chair structure surrounding the metal atom impurity—has emerged from our extensive investigations of silicon clusters in combination with a Cu atom ($CuSi_N$) as the likely ground-state structure of $CuSi_{12}$. These results suggest the systematic importance of Si_{12} cages derived from regular structures with D_{6h} geometry for the architecture of silicon clusters containing metal atom impurities. In the present comparative study, we discuss the salient features of endohedral MSi_{12} clusters with $M=$Cu, Mo, W, as well as several cationic and anionic species of these systems, with regard to their geometric and electronic structure. The interaction between the Si_{12} cage and the enclosed metal impurity is characterized as strongly delocalized bonding for $M=$Mo, W, while Cu tends to form directed bonds with selected atoms of the cage. Linear extension of the MSi_{12} (Me=Mo,W) cells along their principal axes leads to units of the form M_2Si_{18}.

DOI: 10.1103/PhysRevB.67.035426 PACS number(s): 61.46.+w, 31.15.Dv, 36.40.Cg, 73.22.−f

I. INTRODUCTION

Numerous research efforts, both experimental and computational, have been devoted to the understanding of silicon clusters (Si_N).[1,2] The interest in these species is motivated partly by the desire to gain fundamental insight into the mechanisms that govern the evolution of Si systems from the molecular to the macroscopic scale. In addition, there is the prospect of technological innovation through the fabrication of novel materials with Si_N clusters as building blocks. In both respects, the investigations of Si_N have been guided by dramatic developments in the field of carbon clusters C_N during the last two decades. However, no fullerene like architectures have been identified noncontroversially for Si_N units to this date. This disparity between Si_N and C_N is attributed to the finding that the bonding in fullerenes is characterized by sp^2 hybridization, which is more favorable for C_N than for Si_N units.[3]

However, from the extensive knowledge accumulated on a wide variety of metal-doped fullerene species, such as La@C_N ($N=60,74,82$),[4] it has been suggested that implantation of a metal impurity into a Si_N unit could lead to the formation of a cagelike Si_N structure of extraordinary stability.[5] This consideration provides strong motivation for the study of mixed metal-Si clusters.

Several recent experimental projects have dealt with these systems. In a pioneering mass spectrometric investigation using a laser vaporization technique,[6] Beck demonstrated the existence of small mixed transition-metal (TM)-Si clusters, observing various species of the form $TMSi_N$ with TM =Cr,Mo,W; $N=16,17,18$. Additionally, he reported the observation of $CuSi_N$ clusters with a pronounced abundance maximum at $N=10$. This latter study was complemented more recently by experiments of Scherer *et al.*[7] who identified several series of smaller Cu_MSi_N clusters. Stimulated by Beck's experimental work, some computational investigations have been performed on selected $TMSi_N$ species with $N=15,17$, for which the systems were subject to hypothetical symmetry constraints.[8] Moreover, a comprehensive study of the geometric and electronic features of $CuSi_N$ has been carried out,[9–12] and the systematics of MSi_N (M =Cr,Mo,W;$N<7$) clusters[13–15] has been explored.

A recent computational study[16] identified numerous cluster species of the form $M@Si_N$ ($M=$Fe,Ru,Os; $N=14$ and $M=$Ti,Zr,Hf; $N=16$). It was shown that some of these clusters display highest occupied molecular orbital and lowest unoccupied molecular orbital (HOMO-LUMO) gaps whose magnitudes are indicative of extraordinary stability.

The latest experimental achievement related to metal-Si_N clusters was reported by Hiura *et al.*[17] The authors used an ion trap procedure to detect a cluster series of the form MSi_N^+ ($M=$Hf,Ta,W,Re,Ir,…; $N=9,11,12,13,14$). The method makes possible the recording of time-resolved mass spectra and the observation of the growth of a MSi_N^+ cluster species in considerable detail. The products WSi_NH_x of the reaction of W^+ ions with SiH_4 gas molecules were monitored in a temporal sequence of spectra. The growth process of the species slows down for $N>8$ and terminates at $N=12$. At this number of constituents, a saturation point appears to be reached; the capacity of the metal ion to bind additional Si atoms seems to be exhausted. This tendency in conjunction with the observation that the resulting WSi_{12}^+ cation is dehydrogenated suggests that a highly compact cluster is formed in which the W atom occupies an endohedral site. This result can be counted as the first experimental evidence for the existence of a cagelike Si_N frame encapsu-

lating a metal atom. From an extensive geometric search, using a variety of quantum chemical procedures, a regular hexagonal prism with a W atom at the center was identified as the lowest-energy structure for both WSi_N and WSi_N^+.[17]

In a recent computational effort that focused on clusters of the form $CuSi_N$ with $N<13$,[12] the $CuSi_{12}$ unit was characterized and shown to adopt a ground-state geometry closely related to the one proposed for WSi_{12}. More specifically, the $CuSi_{12}$ cluster has been demonstrated to form a cagelike geometry with the Cu impurity enclosed by two deformed hexagonal Si_6 rings. These hexagons bear strong similarity to the Si_6 ''chair geometry,'' which is a structural element of the sp^3-bonded diamond network of solid Si. The WSi_{12} geometry of symmetry group D_{6h} can therefore be interpreted as a regularization of the C_{2h} structure found for $CuSi_{12}$. Note that in our studies of $CuSi_N$, the intuitive assumption of endohedral impurity sites was subjected to critical examination, leading to the conclusion that for Cu in combination with Si_N, exohedral adsorption or substitutional sites are more strongly favored as impurity locations than highly coordinated center sites, provided the number of Si cluster constituents is lower than a certain threshold value which was found to be $N=12$. This result gives additional emphasis to the ''magic'' number 12. It will be interesting to investigate if this atom count remains the smallest number of Si constituents required to establish an endohedral MSi_N unit.

The purpose of the present study is the exploration of salient features related to the geometric, electronic, and magnetic structure of Si_{12} clusters with endohedral metal impurities. We focus on the metal elements Cu, Mo, and W, which we have studied previously as atomic impurities in various Si_N matrices,[9–15] and investigate the interaction between the metal core and the Si_{12} framework with the goal of characterizing the nature of the bonding between both components for each of the systems included.

We will further ask for a possible linear extension of the regular MSi_{12} (M=Mo,W) species in the direction of the principal axes of these units and propose a novel cluster type of the form M_2Si_{18} (M=Mo,W), a three-layered double-hexagonal prism (Si_6-M-Si_6-M-Si_6). This final segment of our study is intended to stimulate research, both computational and experimental, on one-dimensional metal-atom-filled Si nanowires, as the prototype M_2Si_{18} (M=Mo,W) could possibly provide a basic cell for these linear structures. Obviously, this topic assumes major importance in the context of the recent discussion about Si nanotubes,[18] since the metal atom impurities may be found to have an equally stabilizing effect on Si_N tube structures as on closed-shell Si_N cages.

II. METHOD

In this work, we perform density functional theory (DFT) computations based on the hybrid UB3LYP functional which consists of a combination of Becke's exchange functional B3 (Ref. 19) with the nonlocal functional of Lee, Young, and Parr (LYP).[20] Acknowledging the nonzero spin of most of the species investigated, the spin-unrestricted formalism (U) has been applied. Using this procedure, we carried out geometry optimizations for every species considered employing the program GAUSSIAN98.[21] In each case, the stability of the resulting structure has been secured through vibrational analysis. In the following section, we discuss the electronic structure of any one of the obtained equilibrium geometries in terms of the natural electron population.[22] This choice is dictated by numerous cases where Mulliken population analysis was found unreliable, leading, for instance, to a wrong sign for the effective charge of Cu in $CuSi_N$.[9]

Since our investigation includes some negatively charged species—namely, the anion and dianion of Si_{12} as well as the anion of WSi_{12}—we mention that questions have been raised concerning the capacity of DFT-based local approaches to represent systems of net negative charge adequately.[23] This problem, however, which originates from the imperfect cancellation of the electron self-energy in local approximations to the energy functional, is less serious for the hybrid B3LYP procedure. Further, small molecules are expected to be more susceptible to this deficiency than the rather large units discussed in the present context, since the electronic self-repulsion is reduced as the spatial extension of the charge distribution increases. We also remark that no evaluation of electron affinities, for which the indicated shortcoming of local DFT-based procedures should be most pronounced, is attempted in this contribution.

A considerable reduction of the computational effort required for the description of cluster systems is achieved through the application of the effective core potential (ECP) method. The use of an appropriate all-electron basis set for M=Mo,W would make the geometry optimization of the MSi_N (N=12,18) clusters considered here an extremely time-consuming effort, as the high atomic numbers of the metal atoms necessitate a relativistic treatment. On the other hand, it has been shown that the double-zeta LanL2DZ ECP basis set as described in Refs. 24 and 25, which includes scalar relativistic effects, has been shown to generate results of very satisfactory quality for a wide variety of metal-atom-containing systems. This method yields for the bond length of Cu_2 a value of 2.26 Å, which deviates from the experimental finding, R(Cu-Cu)=2.22 Å,[10] by less than 2%. For Cr_2 a bond length of 1.61 Å (Ref. 13) is found, which is well compatible with the experimental result of 1.68 Å (Ref. 26).

Investigating some energy-related quantities on the basis of the LanL2DZ ECP approach, we found a value of 7.82 eV for the ionization potential of Cu and 7.93 eV for that of Cu_2. This is to be compared with experimental results[27] of 7.72 and 7.90 eV, respectively. An all-electron B3LYP/6-311+G(d) calculation yields 8.04 and 8.00 eV, respectively, for these two quantities, diminishing the agreement between measurement and computation, as obtained on the LanL2DZ ECP level.

The ECP approach used in the present context subdivides the electronic system of the W atom into a core consisting of the K, L, M, and N shells and a $5s^25p^65d^46s^2$ valence region described by three basis functions of s character, three p and two d basis functions. For Mo, the configuration $4s^24p^64d^55s^1$ forms the valence region. Likewise, the Si core comprises the K and L shells, and two s as well as two p basis functions, corresponding to the $3s^23p^2$ system, de-

fine the valence region. The valence region of Cu is given by $3s^2 3p^6 3d^{10} 4s^1$, described by three *s*, three *p*, and two *d* functions.

For further testing of our approach, we carried out several geometry optimizations on pure Si_N clusters, comparing with the intensely studied and well-confirmed ground-state structures of these units.[28–30] This examination of equilibrium bond lengths and angles leads to deviations of typically 1%–4%. For some Si_N units, we computed ionization potentials using the B3LYP/LanL2DZ ECP approach and found it comparable with our B3LYP/6-311+G(d) results. Thus we arrived at values of 8.04 eV using the former and 7.88 eV using the latter method for the ionization potential of Si_4. Experimentally, it has been determined that the ionization potential of Si_4 should fall into the range of 7.97–8.49 eV,[31] which is well compatible with the ECP result.

In order to examine the compatibility of the present pseudopotential procedure with the all-electron treatment previously applied, using a basis of the 6-311+G(d) type, in the description of $CuSi_N$ ($N=4,6,8,10,12$),[9–12] we compared the geometry optimization results obtained by the two methods for the ground-state structure of $CuSi_{12}$. Both procedures lead to the same C_{2h} geometry, with small deviations, not exceeding 2% in the Cu-Si and Si-Si bond lengths.

We have secured the dynamic stability of all optimized structures reported in Sec. III by frequency analysis.

III. RESULTS AND DISCUSSION

In the following, we first discuss our findings for the pure Si_{12} matrix in various charge states, then describe individual MSi_{12} (M=Cu,Mo,W) clusters, and conclude with a characterization of extended M_2Si_{12} systems.

A. Si_{12} cage structures

Imposing D_{6h} symmetry on Si_{12}, as shown in Fig. 1(a), subjecting this unit to a self-consistent field (SCF) treatment and inspecting the succession of molecular orbitals, one finds that the HOMO of Si_{12} (D_{6h}) is a half-filled orbital of E_{2g} symmetry. This result implies that Si_{12} (D_{6h}) can be stable only as an open-shell system; i.e., the two alternative E_{2g} orbitals each have to be occupied by one electron. Following Hund's rule, one expects both electrons to have equal spin orientations, corresponding to a spin-triplet arrangement. However, optimization of Si_{12} with the D_{6h} structure defining the initial geometry shows that this species will distort to adopt a characteristic ''double-chair'' arrangement of C_{2h} symmetry displayed in Fig. 1(b). We point out that this unit represents a dimer consisting of two deformed hexagonal Si_6 rings, which may be interpreted as fragments of bulk silicon. This ''chair structure'' has been identified as a stable isomer of Si_6,[28] being higher in energy than the C_{2v} ground state of Si_6 by a difference of $E=5.55$ eV, as evaluated at the MP2/6-31G* level. The relevance of the double-chair structure realized for Si_{12} as a result of relaxation from the initial D_{6h} geometry is further emphasized by the observation that this structure top-capped by one additional Si atom defines an isomer of Si_{13} with C_{3v} symmetry as obtained by B3LYP/6-311+G(d) analysis.[12]

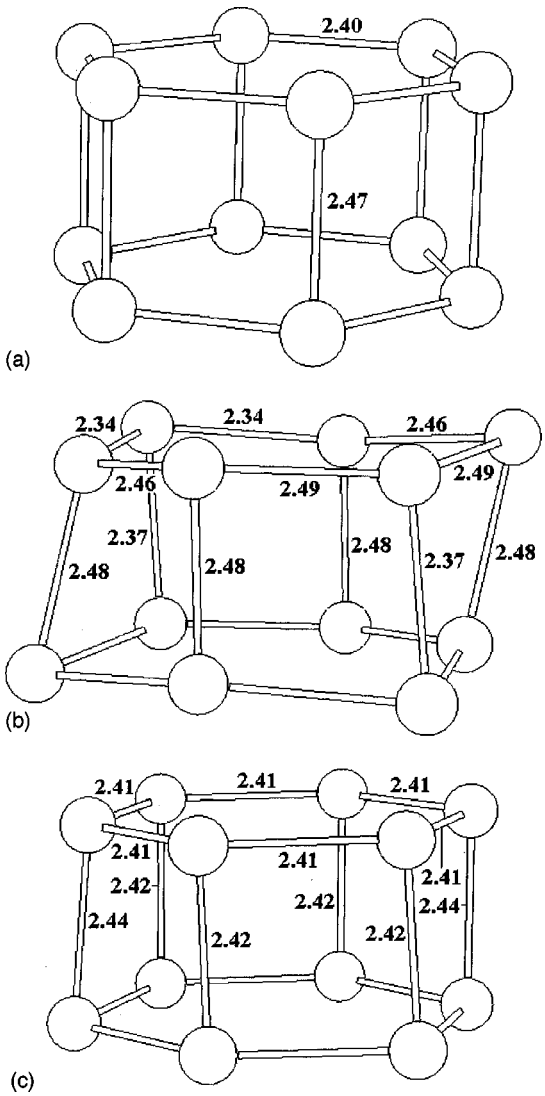

FIG. 1. (a) Geometry of Si_{12} with imposed D_{6h} symmetry. This is the initial structure chosen for our geometry optimization of Si_{12}. (b) Optimized geometry of Si_{12}, a ''double-chair'' C_{2h} structure. (c) Optimized geometry of Si_{12}^{2+}, approaching D_{6h} symmetry. In all three cases, bond lengths are indicated in units of Å.

As is obvious from the character of the Si_{12} (D_{6h}) HOMO indicated above, this unit could alternatively be occupied by two electrons with opposite spin orientations. It should be emphasized that the resulting state is not a spin eigenstate, but a broken symmetry solution. As allowance is made for relaxation, Si_{12} (D_{6h}) distorts from this initial state to adopt again a double-chair structure comparable to the equilibrium geometry of the Si_{12} spin triplet. From the atomization energies listed in Table I, it is seen that the Si_{12} spin triplet has slightly higher stability than the corresponding spin singlet, their ground state energies differing by the small but noticeable amount of 0.24 eV. We note that the term ''triplet'' is employed here for the sake of a distinction between the two alternative states investigated, but is not to be taken in the literal sense, as the spin-unrestricted formalism is used in the

TABLE I. Electronic properties of neutral and charged Si_{12} cage structures. All energies are given in eV.

Si_{12} system	Spin	ΔE_b[a]	ΔE_{HL}[b]
Si_{12}^{2+}	0	1.17	1.42
Si_{12}^{+}	1/2	2.79	
Si_{12}	0	2.67	1.11
Si_{12}^{-}	1/2	3.01	
Si_{12}^{2-}	0	3.06	2.82
Si_{12}	1	2.69	

[a]Binding energy per cluster constituent.
[b]HOMO-LUMO energy difference. This quantity is only indicated for spin-singlet states.

computation of this solution. The spin contamination for the Si_{12} state labeled triplet, however, is extremely small, amounting to less than one per mille.

As a further possibility to prevent the described symmetry reduction of the Si_{12} unit, we discuss the removal of the ambiguity associated with the incompletely filled E_g HOMO of Si_{12} (D_{6h}) through addition or subtraction of two electrons to or from this electronic level. Following this strategy, one will produce a dianion in the former case and a dication in the latter one. Commenting first on Si_{12}^{2-}, we detect again a considerable degree of distortion in the equilibrium geometry which can still be understood as a double-chair structure. In contrast, Si_{12}^{2+} stabilizes as a near-regular hexagonal prism [see Fig. 1(c)] and thus indeed approaches the limit of D_{6h} symmetry, thereby differing markedly from the structural paradigm set by the shape of Si_{12}. Further inspection of charged versions of Si_{12}—namely, Si_{12}^{+} and Si_{12}^{-}, which both prefer a double-chair arrangement—leads to the conclusion that Si_{12}^{2+} constitutes a structural exception within this cluster group.

We point out that, as expected, the HOMO-LUMO energy differences for Si_{12}^{2+} and Si_{12}^{2-} turn out to be markedly higher than that found for Si_{12} (see Table I). This effect is particularly pronounced in the case of Si_{12}^{2-}.

B. MSi$_{12}$ (M=Cu,Mo,W)

The observations reported in the preceding paragraphs hint at the role that charge transfer may play in defining the geometries of $M@Si_{12}$ clusters. More specifically, upon insertion of a metal atom into a Si_{12} (D_{6h}) cage, electron transfer is expected to occur between the metal impurity and the Si_{12} frame. Our investigation of the Si_{12} units that arise from the relaxation of an original structure constrained by D_{6h} symmetry makes possible a qualitative prediction of a correlation between the final cage geometry and the charge state of the enclosed metal impurity. For neutral, singly cationic, or anionic as well as dicationic metal species, the Si_{12} cage appears likely to stabilize as a double-chair structure. If, however, the dianionic state of the metal impurity is realized, small or zero relaxation from the initial D_{6h} structure is likely.

We tested this model by an exploration of two MSi_{12} species—namely, $CuSi_{12}$ and WSi_{12}. Foregoing research has established that Cu as impurity in Si_N clusters tends to act as an electron donor,[9,10] while W behaves as an electron acceptor in the ground states of all WSi_N examined so far.[15] For both cases, we performed geometry optimizations, placing initially the respective metal atom at the center site of a Si_{12} (D_{6h}) frame. We arrived at the structures displayed in Figs. 2(a) and 2(b). Whereas for $CuSi_{12}$ the Si_{12} cage distorts into a double-chair arrangement of C_{2h} symmetry, the initial D_{6h} symmetry is retained for WSi_{12}. It is pointed out that the two structures shown in Figs. 2(a) and 2(b) can be regarded as realistic candidates for the ground-state geometry of the respective MSi_{12} species. The proposed equilibrium structure of $CuSi_{12}$ has been determined to be lowest in energy among numerous plausible geometries by an extensive search of the $CuSi_{12}$ potential energy surface[12] and particularly by a careful examination of units that can be generated by insertion of Cu into the Si_{12} (C_s) ground-state structure emerging from B3LYP/6-311+G(d) computation. Moreover, possible surface positions of Cu, such as adsorption sites or substitutional sites within the Si_{13} matrix, have been included in this comparison (see Sec. I). Similarly, Hiura *et al.* have identified the WSi_{12} geometry shown in Fig. 2(b) as the most stable among a large number of alternatives by various quantum chemical procedures.[17]

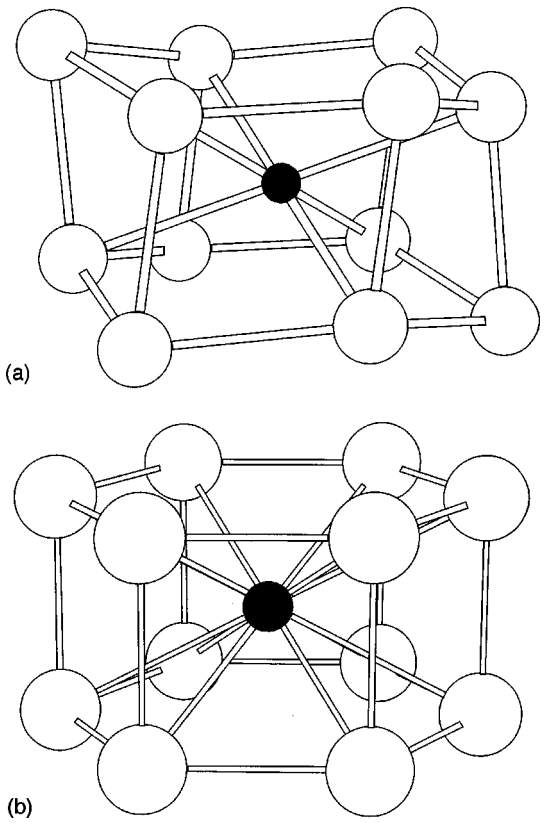

FIG. 2. (a) Optimized geometry of $CuSi_{12}$, a C_{2h} structure. (b) Optimized geometry of WSi_{12}, a D_{6h} structure.

In an attempt to relate the different Si_{12} cage geometries of $CuSi_{12}$ and WSi_{12} to the charge transfer characteristics of these units, we computed the natural charges of the metal atom impurities and found 0.48 for Cu and −1.74 for W. Although the values of the natural charge should be under-

stood as indicative of a qualitative trend rather than as numerically reliable results, these findings clearly reflect the expected reversal of the direction of electron transfer from $M=$Cu to $M=$W. Considering these natural charges on the metal impurities in the light of our above remarks related to the structures of neutral or negatively charged Si_{12} cages, one will expect the formation of a Si_{12} double-chair frame for the $CuSi_{12}$ species. The natural charge on W, in contrast, is compatible with an effective dianion charge state of W, and thus the Si_{12} cage may be best described as Si_{12}^{2+} for WSi_{12}, corresponding to a restoration of D_{6h} symmetry of Si_{12}, driven by electron transfer from the cage to the central impurity.

This hypothesis gains additional support from a comparative study of the HOMO's of Si_{12}^{-} and $CuSi_{12}$ as well as Si_{12}^{2+} and WSi_{12}, as presented in Figs. 3(a), 3(b) and 4(a), 4(b), respectively. Obviously, the HOMO's for both MSi_{12} clusters can be interpreted as those of the charged Si_{12} units, i.e., Si_{12}^{-} and Si_{12}^{2+}, combined with an admixture due to the metal core. This suggests that, to a certain approximation, the units $CuSi_{12}$ and WSi_{12} may be understood as $Cu^{+}Si_{12}^{-}$ and $W^{2-}Si_{12}^{2+}$. We conclude that electron transfer contributes substantially to the stabilization of these species.

The HOMO of $CuSi_{12}$ appears as a mere addition of that of Si_{12}^{-} and a contribution stemming from a Cu^{+} core, represented by the clearly visible atomic *d* orbital shape at the center of the distribution shown in Fig. 3(b). No interaction is found between the Si_{12} and Cu components of the HOMO. In contrast, the HOMO of WSi_{12} [Fig. 4(b)] is indicative of covalent bonding between the metal impurity and the Si_{12} cage atoms. A similar profile—namely, a strongly delocalized *M*-Si ligand interaction—is encountered in the HOMO-1 of $CuSi_{12}$.

The LUMO of WSi_{12} [see Fig. 4(c)] displays a construction principle reminiscent of that of the $CuSi_{12}$ HOMO. The metal core of WSi_{12}, consisting of a strongly pronounced $W(D_0)$ orbital, is embedded into a regular electronic cage structure of sixfold symmetry, and these two components are antibonding. The marked contrast between the two frontier orbitals of WSi_{12} corresponds to a high HOMO-LUMO energy gap of 2.59 eV (see Table III, below).

From our studies of the molecular orbital profiles of $CuSi_{12}$ and WSi_{12} as well as the respective charge density distributions, we conclude that Cu(W) in $Cu(W)Si_{12}$ is 6fold (12fold) coordinated. This finding agrees with the geometric data of MSi_{12} listed in Table II, where two *M*-ligand distances are indicated for $M=$Cu, while only one distance exists for $M=$W.

$MoSi_{12}$ exhibits an architecture strictly analogous to that of WSi_{12}. This is not surprising since Mo and W belong to the same group of the periodic table. It is remarkable, however, that the distance parameters of the Si_{12} (D_{6h}) cage only undergo minimal alterations when W is replaced by Mo (see Table II). The vertical separation between the two Si_6 hexagons changes from 2.47 Å in WSi_{12} to 2.46 Å in $MoSi_{12}$, and the distance between adjacent Si atoms in either of the two Si_6 rings changes from 2.405 to 2.407 Å. The natural charge on the endohedral Mo impurity is determined to be

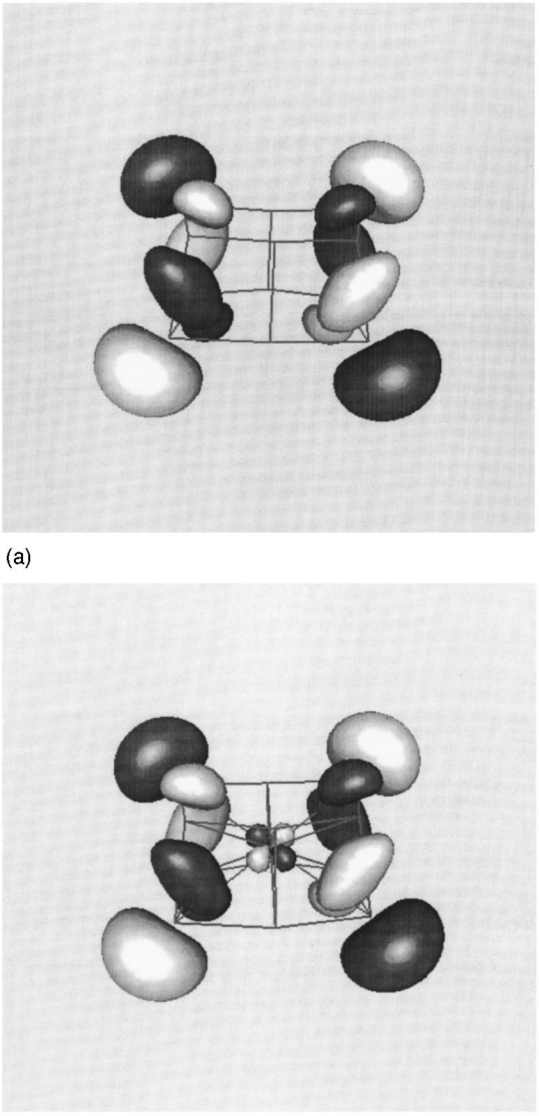

(a)

(b)

FIG. 3. (a) Representation of the Si_{12}^{-} HOMO. (b) Representation of the $CuSi_{12}$ HOMO. In both cases, an isosurface parameter of magnitude 0.03 has been chosen. The dark zones correspond to positive, the bright zones to negative values of the respective orbital function.

$-1.65e$ and thus deviates by 7% from the corresponding value for W in WSi_{12} (see above).

A more meaningful criterion of stability of MSi_{12} ($M=$Cu,Mo,W) systems than the binding energy is the embedding energy ΔE_e. This quantity is defined as the energy release upon implantation of the metal atom into the Si_{12} cage and is given by

$$\Delta E_e = E(MSi_{12}) - E(M) - E(Si_{12}),$$

where the energies of the species involved are evaluated at their equilibrium geometries. The results for $\ni E_e$ in Table III establish a natural hierarchy among the clusters compared. The values range from 0.83 eV per Si cage atom for $M=$W to 0.32 eV per Si cage atom for $M=$Cu. The marked

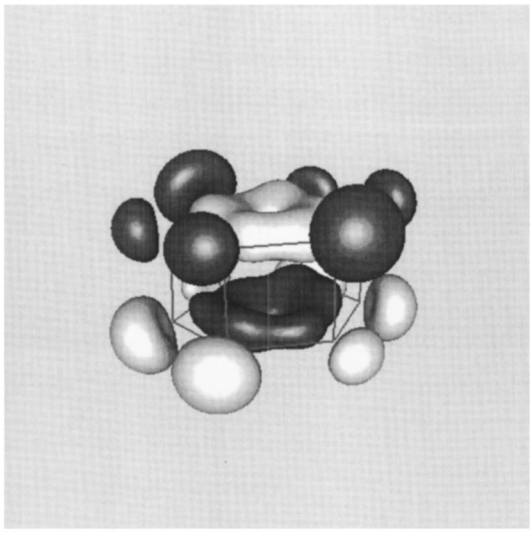

(a)

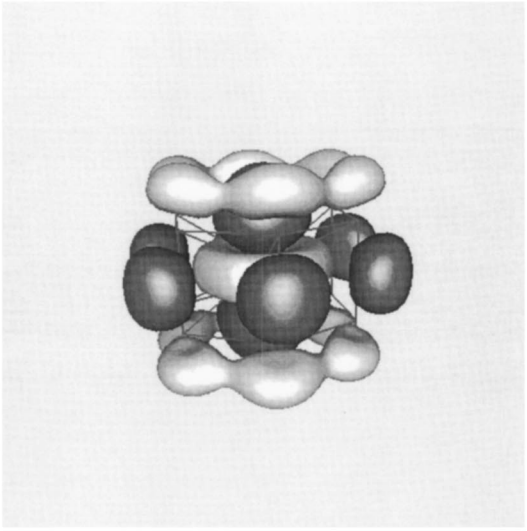

(c)

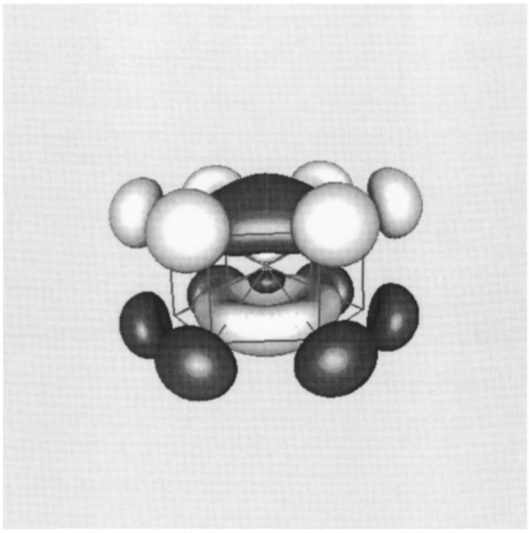

(b)

FIG. 4. (a) Representation of the Si_{12}^{2+} HOMO. (b) Representation of the WSi_{12} HOMO. (c) Representation of the WSi_{12} LUMO. In all three cases, an isosurface parameter of magnitude 0.03 has been chosen. The dark zones correspond to positive, the bright zones to negative values of the respective orbital function.

drop of $\ni E_e$ from WSi_{12} to $CuSi_{12}$ is ascribed to the finding that the coordination of Cu as an impurity in Si_{12} is only half as large as the coordination of W in the system, implying markedly smaller cage stabilization by Cu than by W. Also note that the WSi_{12} embedding energy is comparable to the largest values of this quantity identified in Ref. 16 for systems of the form MSi_{14} and MSi_{16}. The ΔE_e results reported there range from 0.70 to 1.00 eV. The WSi_{12} system, however, represents a conjunction of a sizable embedding energy and an extraordinarily high HOMO-LUMO gap. These facets combined account, in our view, for the experimentally affirmed exceptional stability of this cluster species.

From geometry optimizations for the singly positive species $MoSi_{12}^{+}$ and WSi_{12}^{+}, we evaluated the adiabatic ionization potentials (AIP's) for both cluster types. The resulting MSi_{12}^{+} (M=Mo,W) systems have D_{6h} symmetry and the bonding characteristics of the respective neutral clusters. As can be seen from Table III, only a small difference (ΔAIP) of 0.13 eV is found, which is in the 2% range. This value is substantially smaller than the experimental result for the difference of the atomic AIP's of W and Mo—namely, 0.59 eV (Ref. 32)—which makes it appear unlikely that the AIP's of the MSi_{12} clusters should be predominantly determined by the metal atom species. Instead, the surprising constancy of the Si_{12} framework in MSi_{12} (M=Mo,W) as well as the near identity of the bonding patterns in both cases seems to be the main cause of the observed similarity of the AIP's in both units.

Our geometry optimization of the WSi_{12}^{-} anion leads to another D_{6h} structure. The natural charges on the constituents of WSi_{12} amount to $Q(W)=-2.18e$ and $Q(Si)=+0.10e$ and thus suggest that the charges are distributed over the Si_{12} frame and the metal impurity according to the qualitative scheme $W^{2-}Si_{12}^{+}$.

In view of the high spin multiplicity of the W atom which adopts a $^5D_3$ ground state, the most stable WSi_{12} isomer may exhibit nonzero spin. Following this consideration, we investigated the triplet ($S=1$) state of WSi_{12}, which, as MSi_{12} (M=Mo,W) in the singlet ($S=0$) state, stabilizes in D_{6h} symmetry. While we found nearly vanishing differences

TABLE II. Geometric properties of MSi_{12} (M=Cu,Mo,W) including the charged MSi_{12} species discussed in Sec. III. All values are given in Å.

MSi_{12}	Spin	Symmetry group	$D(M\text{-Si})^a$	$D(Si_6\text{-}Si_6)^b$	$D(\text{Si-Si})^c$
$CuSi_{12}$	1/2	C_{2h}	2.49, 2.50		
$MoSi_{12}$	0	D_{6h}	2.70	2.46	2.407
$MoSi_{12}^+$	1/2	D_{6h}	2.72	2.43	2.429
WSi_{12}	0	D_{6h}	2.70	2.47	2.405
WSi_{12}^+	1/2	D_{6h}	2.71	2.435	2.426
WSi_{12}^-	1/2	D_{6h}	2.71	2.48	2.407
WSi_{12}	1	D_{6h}	2.71	2.44	2.423

[a]Distance M-Si. In the case of $CuSi_{12}$, four different bond lengths exist; the shortest are indicated.

[b]Vertical distance between the two regular Si_6 hexagons in the D_{6h} structures.

[c]Distance between adjacent Si atoms in each of the two Si_6 hexagons.

between the distance parameters for the two examined spin-singlet units, deviations of about 1% between the vertical separations of the two Si_6 planes and the next-neighbor distances within a Si_6 ring are noticed comparing WSi_{12} ($S=1$) with WSi_{12} ($S=0$), as is documented in Table II. The total energy of the triplet is found to be higher than that of the singlet by the substantial amount of $\Delta E=1.25$ eV (see Table III), which makes it appear likely that the most stable isomer of WSi_{12} has spin-singlet character.

C. M_2Si_{18} (M=Mo,W)

Extending WSi_{12} in the direction of the sixfold axis by another WSi_6 element yields the stable unit W_2Si_{18} shown in Fig. 5. This species consists of a conjunction of two Si_{12} cage structures, each sharing one Si_6 hexagon and containing one W impurity. This combination, however, is not a fusion of two identical WSi_{12} cells. As a result of the interaction between the two W atoms, each is somewhat shifted from the center position of its Si_{12} cage towards the top and bottom Si_6 rings, respectively. This displacement of the impurity location impacts the bonding both between the Si_6 layers and within each of the Si_6 layers. More specifically, we observe a periodic distance change between adjacent Si atoms in each of the three Si_6 rings (see Table IV). A slight contraction of the equilibrium bond length (=2.41 Å) between neighboring Si atoms in the WSi_{12} unit alternates with a more pronounced expansion of this length. This variation reaches a maximum in the intermediate layer which defines a mirror plane for the structure as a whole. The D_{6h} symmetry of the WSi_{12} matrix therefore is reduced to D_{3h} in the derived W_2Si_{18} unit.

TABLE III. Energetic properties of MSi_{12} (M=Cu,Mo,W) including the charged MSi_{12} species discussed in Sec. III. All energies are given in eV.

MSi_{12}	Spin	Symmetry group	$\Delta E_b{}^a$	$\Delta E_e{}^b$	$\Delta E_{HL}{}^c$	AIP[d]
$CuSi_{12}$	1/2	C_{2h}	2.77	0.32		6.59
$MoSi_{12}$	0	D_{6h}	3.07	0.65	2.19	7.66
$MoSi_{12}^+$	1/2	D_{6h}	3.13			
WSi_{12}	0	D_{6h}	3.24	0.83	2.59	7.79
WSi_{12}^+	1/2	D_{6h}	3.29			
WSi_{12}^-	1/2	D_{6h}	3.40			
WSi_{12}	1	D_{6h}	3.14	0.65		6.53

[a]Binding energy per cluster constituent.

[b]Embedding energy per cage atom.

[c]HOMO-LUMO energy difference. This quantity is only indicated for spin-singlet states.

[d]Adiabatic ionization potential.

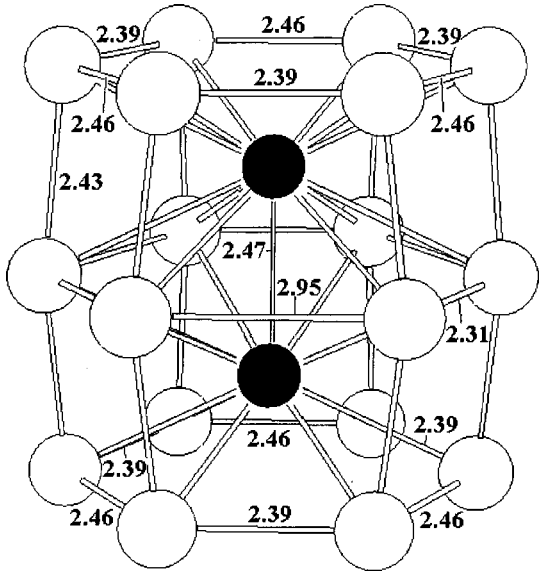

FIG. 5. Optimized geometry of W_2Si_{18}, a D_{3h} structure. Bond lengths are indicated in units of Å.

According to the values listed in Table IV, the equilibrium geometry of $W_2Si_{18}^+$ differs only slightly from that of the neutral species; also, the cation keeps the D_{3h} symmetry of W_2Si_{18}. We point out that $W_2Si_{18}^+$ has been detected by mass spectrometry.[17]

The construction principle of the HOMO of W_2Si_{18} is related to that of the HOMO of WSi_{12} [Fig. 4(b)]. As seen

TABLE IV. Geometric properties of M_2Si_{18} (M=Mo,W) including the charged $M_2Si_{18}^+$ species discussed in Sec. III. All values are given in Å.

M_2Si_{18}	$D(M\text{-}M)^a$	$D(Si_6\text{-}Si_6)^b$	$D(\text{Si-Si})_{long}{}^c$	$D(\text{Si-Si})_{short}{}^c$
Mo_2Si_{18}	2.43	2.41	3.00	2.31
$Mo_2Si_{18}^+$	2.40	2.38	3.12	2.31
W_2Si_{18}	2.47	2.42	3.00	2.31
$W_2Si_{18}^+$	2.47	2.39	3.09	2.30

[a]Distance between the two metal atoms.

[b]Vertical distance between the two adjacent Si_6 hexagons.

[c]Shorter distance between adjacent Si atoms in the intermediate Si_6 layer (see Sec. III).

[d]Longer distance between adjacent Si atoms in the intermediate Si_6 layer (see Sec. III).

TABLE V. Electronic properties of M_2Si_{18} (M=Mo,W) including the charged $M_2Si_{18}^+$ species discussed in Sec. III. All values are given in eV.

M_2Si_{18}	ΔE_b[a]	ΔE_{HL}[b]	AIP[c]
Mo_2Si_{18}	3.16	1.81	6.79
$Mo_2Si_{18}^+$	3.24		
W_2Si_{18}	3.37	1.92	6.94
$W_2Si_{18}^+$	3.44		

[a]Binding energy per cluster constituent.
[b]HOMO-LUMO energy difference. This quantity is indicated only for spin-singlet states.
[c]Adiabatic ionization potential.

there, hybridization of atomic W(p_z) and Si(p_x,p_y) orbitals gives rise to the formation of umbrella structures at the top and bottom of the unit. Likewise, uniform interaction with all constituents of the upper and lower Si_6 hexagons is encountered, as may be inferred from inspection of the electronic charge density distribution. From this analysis, we also find that W_2 is not bonded to any element of the intermediate Si_6 ring, which is segmented into three clearly separated Si_2 subunits.

The two W atoms are connected by a strongly stretched covalent bond with bond length of 2.47 Å. This value is to be compared with the equilibrium bond length of the free W_2 molecule of 2.19 Å at the UB3LYP/LanD2Z computational level used in this work. This sizable bond elongation appears plausible in view of the finding that each of the W atoms interacts with the top or bottom Si_6 layer, but no bond is established between any W atom and the intermediate Si_6 layer. Instead, a W-W bond is formed which is substantially strained as a consequence of the attraction of each W atom by the terminating Si_6 layer to which it attaches itself.

As in the case of MSi_{12} (M=Mo,W), the structural features of W_2Si_{18} and Mo_2Si_{12} are strictly analogous. Again, the geometries of the two complexes exhibit striking quantitative similarities, as the deviation between equivalent Si-Si bond lengths in W_2Si_{18} and Mo_2Si_{18} are found to be less than 1%. Although the ionization potentials listed in Table V for both these units differ more from each other than the comparable values determined for MSi_{12} (M=Mo,W), this difference is still so small that the metal impurity cannot be their primary origin.

In the context of our discussion of M_2Si_{12} (M=W,Mo) units, we point out that a recent publication[33] deals with the interaction between two WSi_{12} clusters, using the B3LYP/LANL2DZ formalism employed in this work. The authors conclude that stacking two WSi_{12} clusters along the sixfold axis does not result in a stable $(WSi_{12})_2$ geometry. However, linking both WSi_{12} units by a W spacer atom leads to an equilibrium structure of the form W_3Si_{24}. A cluster of this composition may be generated from the W_2Si_{18} unit discussed here by the addition of another WSi_6 segment. The authors argue that the species thus attained is metastable, making it appear unlikely that W-metal-filled silicon nanowires could be constructed by mere stacking of WSi_{12} units linked together by W atoms.

In summary, a comparative study of the geometric, electronic, and magnetic properties of the systems MSi_{12} (M=Cu,Mo,W) and related species has been performed. We investigated systematically the architecture of MSi_{12} (M=Cu,Mo,W), acknowledging that WSi_{12} stabilizes in D_{6h} symmetry. Thus, as the first step of our research, we analyzed the pure Si_{12} (D_{6h}) cage, which turned out to be an open-shell system that distorts into a C_{2h} structure. This system can be characterized as the combination of two Si_6 units with chair geometry. Implanting a W impurity into the Si_{12} (D_{6h}) cage, we observed a shell-closing effect related to substantial electron transfer from the cage to the endohedral impurity, resulting in a stable D_{6h} structure. A strictly analogous behavior is recorded for M=Mo. However, if Cu is chosen as impurity species, the C_{2h} double-chair structure emerges as equilibrium geometry. This contrasting behavior of the systems compared is ascribed to the finding that the electron transfer between the metal atom and the Si_{12} frame not only reverses its direction, but also weakens substantially as one goes from M=Mo,W to M=Cu. In the latter case, shell closing is not achieved any more under the D_{6h} constraint, and the system distorts.

The electron transfer model between the Si_{12} cage and the metal atom core is substantiated through natural charge analysis as well as a comparison between the HOMO's of MSi_{12} and Si_{12} in various charge states. The latter examination yields the near identity of the HOMO of Si_{12}^{2+} and the contribution of Si_{12} to the HOMO of WSi_{12}. Analogous results are found for Si_{12}^- and $CuSi_{12}$.

Exploring the electron charge density distribution of MSi_{12} (M=Cu,W), we observed that W tends to form a highly delocalized bond with the Si_{12} cage, interacting uniformly with all Si atoms. In contrast, Cu forms directed and selective bonds, which accounts for the detected symmetry reduction of the cage in $CuSi_{12}$. The pronounced stability of the WSi_{12} unit is documented by the finding that both its embedding energy ΔE_e and its HOMO-LUMO gap turn out to be largest in the MSi_{12} (M=Cu,Mo,W) series.

The prototypical $W(Mo)Si_{12}$ structure can be linearly continued along the sixfold axis of the cluster, which leads to $W(Mo)_2Si_{18}$. The original D_{6h} symmetry is reduced to D_{3h} in this extended unit. The two W atoms interact with the top or bottom Si_6 layer, respectively, and form a considerably lengthened covalent bond between each other.

IV. CONCLUSION

Based on the findings described in Sec. III, it should be interesting to investigate further metal impurities at center sites of small Si_N clusters and to address the question suggested by our computational work on $CuSi_N$ (Ref. 12) as well as the experimental data reported by Hiura *et al.*[17] Namely, is MSi_{12} a member of a ''magic'' series of endohedral M_MSi_N clusters with extraordinary stability? And if so, what is the growth pattern of this series? A recent computational investigation[34] on the system $IrSi_9^+$, which belongs to the detected cluster sequence, demonstrated that an endohedral D_{3h} structure exceeds the stability of exohedral alternatives by a substantial amount. Currently, we continue the search

for regular endohedral MSi_N units, corresponding to the terminal units identified by mass spectrometry.[17]

A different class of questions is raised by the observations associated with M_2Si_{18} (M=Mo,W). Although the existence of silicon counterparts of metal-loaded carbon nanotubes built from MSi_{12} as cellular element appears questionable in view of the differences between carbon and silicon chemistry and the observed metastability of a stacked WSi_{12}-W-WSi_{12} compound,[33] our work demonstrates that a limited linear extension of MSi_{12} is possible, giving rise to units of pronounced stability. In parallel to our research on MSi_N, we are currently exploring the conditions for encapsulation of various metal dimers by stacked silicon cages. Further, on the basis of the results described here, it seems worthwhile to examine the interaction of two M_2Si_{18} (M=Mo,W) clusters, attempting to address the critical question for a potential transition from the finite to the periodic one-dimensional case from a different perspective than has been done so far. Such research is being initiated in our laboratories.

ACKNOWLEDGMENT

The support given to this work by the National Science Foundation (NSF) through the CREST program (Grant No. HRD-9805465) is gratefully acknowledged.

[1] M. F. Jarrold, Science **252**, 1085 (1991); A. Shvartsburg, M. Jarrold, B. Liu, Z.-Y. Lu, C.-Z. Wang, and K.-M. Ho, Phys. Rev. Lett. **81**, 4616 (1998).
[2] I. Rata, A. Shvartsburg, M. Horoi, T. Frauenheim, K. W. M. Siu, and K. Jackson, Phys. Rev. Lett. **85**, 546 (2000); L. Mitas, J. C. Grossman, I. Stich, and J. Tobik, *ibid.* **84**, 1479 (2000).
[3] M. Menon and K. R. Subbaswamy, Chem. Phys. Lett. **219**, 219 (1994).
[4] R. E. Smalley, in *Fullerenes*, edited by G. S. Hammond and V. J. Kuck, ACS Symposium Series No. 481 (Washington, D.C., American Chemical Society, 1992), p. 141.
[5] K. Jackson and B. Nellermoe, Chem. Phys. Lett. **254**, 249 (1996).
[6] S. M. Beck, J. Chem. Phys. **90**, 6306 (1989).
[7] J. J. Scherer, J. B. Paul, C. P. Collier, and R. J. Saykally, J. Chem. Phys. **102**, 5190 (1995).
[8] J. G. Han and Y. Y. Shi, Chem. Phys. **266**, 33 (2001).
[9] C. Xiao and F. Hagelberg, J. Mol. Struct.: THEOCHEM **529**, 241 (2000).
[10] C. Xiao, F. Hagelberg, I. V. Ovcharenko, and W. A. Lester, J. Mol. Struct.: THEOCHEM **549**, 181 (2001).
[11] I. V. Ovcharenko, W. A. Lester, C. Xiao, and F. Hagelberg, J. Chem. Phys. **114**, 9028 (2001).
[12] C. Xiao, F. Hagelberg, and W. A. Lester, Phys. Rev. B **66**, 075425 (2002).
[13] J. G. Han and F. Hagelberg, Chem. Phys. **263**, 255 (2001).
[14] J. G. Han and F. Hagelberg, J. Mol. Struct.: THEOCHEM **549**, 165 (2001).
[15] J. G. Han and F. Hagelberg, Struct. Chem. **13**, 173 (2002).
[16] V. Kumar and Y. Kawazoe, Phys. Rev. Lett. **87**, 45503 (2001).
[17] H. Hiura, T. Miyazaki, and T. Kanayama, Phys. Rev. Lett. **86**, 1733 (2001).
[18] B. Marsen and K. Sattler, Phys. Rev. B **60**, 11 593 (1999).
[19] A. D. Becke, J. Chem. Phys. **98**, 1372 (1993).
[20] C. Lee, W. Yang, and R. G. Parr, Phys. Rev. B **27**, 785 (1988).
[21] M. J. Frisch, G. W. Trucks, H. B. Schlegel, G. E. Scuseria, M. A. Robb, J. R. Cheeseman, V. J. Zakrzewski, J. A. Montgomery, R. E. Stratmann, J. C. Burant, S. Dapprich, J. S. Millam, A. D. Daniels, K. N. Kudin, M. C. Strain, O. Farkas, J. Tomasi, V. Barone, M. Cossi, R. Cammi, B. Mennucci, C. Pomelli, C. Adamo, S. Clifford, J. Ochterski, G. A. Petersson, P. Y. Ayala, Q. Cui, K. Morokuma, D. K. Malick, A. D. Rabuck, K. Raghavachari, J. B. Foresman, C. Cioslowski, J. V. Ortiz, B. B. Stefanov, G. Liu, A. Liashenko, P. Piskorz, I. Komaromi, R. Gomperts, R. L. Martin, D. J. Fox, T. Keith, M. A. Al-Laham, H. P. Peng, A. Nanavakkara, C. Gonzalez, M. Challacombe, P. M. W. Gill, B. G. Johnson, W. Chen, M. W. Wong, J. L. Andres, M. Head-Gordon, E. S. Replogle, and J. A. Pople, computer code GAUSSIAN 98 (revision A.1), Gaussian, Inc., Pittsburgh, 1998.
[22] J. E. Carpenter and F. Weinhold, J. Mol. Struct.: THEOCHEM **169**, 41 (1988); A. E. Reed, R. B. Weinstock, and F. Weinhold, J. Chem. Phys. **83**, 735 (1985).
[23] N. Rösch and S. B. Trickey, J. Chem. Phys. **106**, 8940 (1997).
[24] P. J. Hay and W. R. Wadt, J. Chem. Phys. **82**, 270 (1985).
[25] W. R. Wadt and P. J. Hay, J. Chem. Phys. **82**, 284 (1985).
[26] S. M. Casey and D. G. Leopold, J. Chem. Phys. **97**, 816 (1993).
[27] P. Calaminici, A. M. Koster, N. Russo, and D. R. Salahub, J. Chem. Phys. **105**, 9546 (1996).
[28] K. Raghavachari, J. Chem. Phys. **84**, 5672 (1986).
[29] R. Fournier, S. B. Sinnott, and A. E. DePristo, J. Chem. Phys. **97**, 4149 (1992).
[30] A. A. Shvartsburg, B. Liu, M. F. Jarrold, and K. M. Ho, J. Chem. Phys. **112**, 4517 (2000).
[31] K. Fuke, K. Tsukamoto, F. Misaizu, and M. Sanekata, J. Chem. Phys. **99**, 7807 (1993).
[32] G. Herzberg, *Atomic Spectra and Atomic Structure*, 2.ed. (Dover, New York, 1944), p. 140.
[33] Q. Sung, Q. Wang, T. Briere, and Y. Kawazoe, J. Phys.: Condens. Matter **14**, 4503 (2002).
[34] F. Hagelberg and C. Xiao, Struct. Chem. (to be published).